Transactions of the **13th International Conference on Structural Mechanics in Reactor Technology** (SMiRT 13), Escola de Engenharia - Universidade Federal do Rio Grande do Sul, Porto Alegre, Brazil, August 13-18, 1995

# Nonlinear numerical analysis of a large compensator

Henkel, F.O., Reuchlein, R., Wölfel, H.
*Wöelfel Beratende Ingenieure, Würzburg, Germany*

## 1 INTRODUCTION

In a nuclear power plant a large compensator serves to radially/axially connect the reactor pressure vessel (RPV) with the surrounding building structure. Since this building structure is supported by neoprene pads the compensator experiences considerable (tangential) horizontal constraining deformation, for additional horizontal load cases.
By means of a numerical investigation using the finite-element method the influences of different methods and parameters of analysis upon the results of deformation, stress and stability analyses shall be demonstrated.
For that purpose linear analyses, linear buckling analyses and various nonlinear analyses considering nonlinear material behaviour, large deformations, geometric imperfections and gaps are compared to each other. The equations which the individual analyses are based on and the differences in the method are compared.

## 2 DESCRIPTION OF MODEL

Figure 1 b shows the location of the reactor pressure vessel (RPV) in the reactor building. In the upper region along its edge the RPV is connected to the reactor pool via a steel seal compensator (cp. Figure 1 a). In order to avoid deflection of the compensator it is freely supported on 12 equally distributed consoles which are fixed at the RPV. The compensator allows an extension of the RPV into the radial direction as well as a displacement free of constraints into the vertical direction. However, due to the tangential stiffness of the compensator a horizontal displacement of the RPV relative to the reactor pool leads to constraining stresses and respective forces of reaction. The horizontal static compensator stiffness in dependence of the relative displacements is determined by means of finite-element analyses. Due to the symmetry/antimetry conditions a quarter model of the compensator can be used for the analyses. Figure 2 shows the FE-model of the compensator with the boundary conditions defined. The model consists of 2790 shell elements (8 nodes, parabolic shape) with 8613 nodes. In the area of the expansion joints inside and outside of the compensator the thickness of sheet is 3 mm. The central part has a thickness of 28 mm. With some of the analyses gap elements were used in the area of the consoles below the compensator. Thus lowering (negative z-direction) is avoided and uplift of the compensator is possible. A constraining displacement of up to 10 mm in the x-direction is applied as loading at all nodes located at the inner ring (RPV connection), which was estimated as maximum relative displacement if the building parts were not connected through the compensator. The bilinear stress-strain relation used with the elasto-plastic analyses is shown in Figure 3. At a strain of 0.2 % the yield stress is 225N/mm$^2$. The modulus of elasticity E in the linear region is 112500 N/mm$^2$, in the plastic region an $E_t$ of 5000 N/mm$^2$ is assumed. If plastic strains appear isotropic hardening is applied.

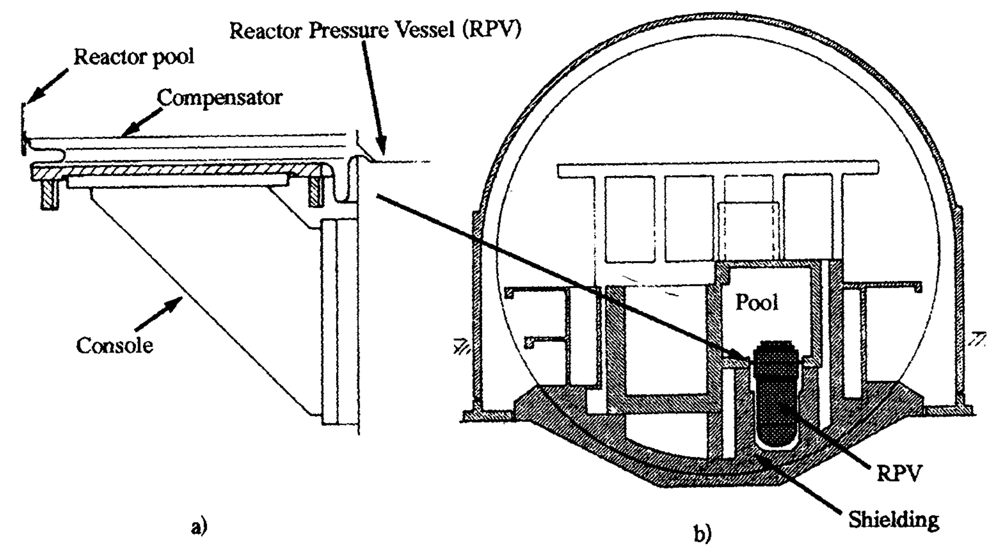


Figure 1. Cut through Compensator (a) and location of RPV in reactor building (b)

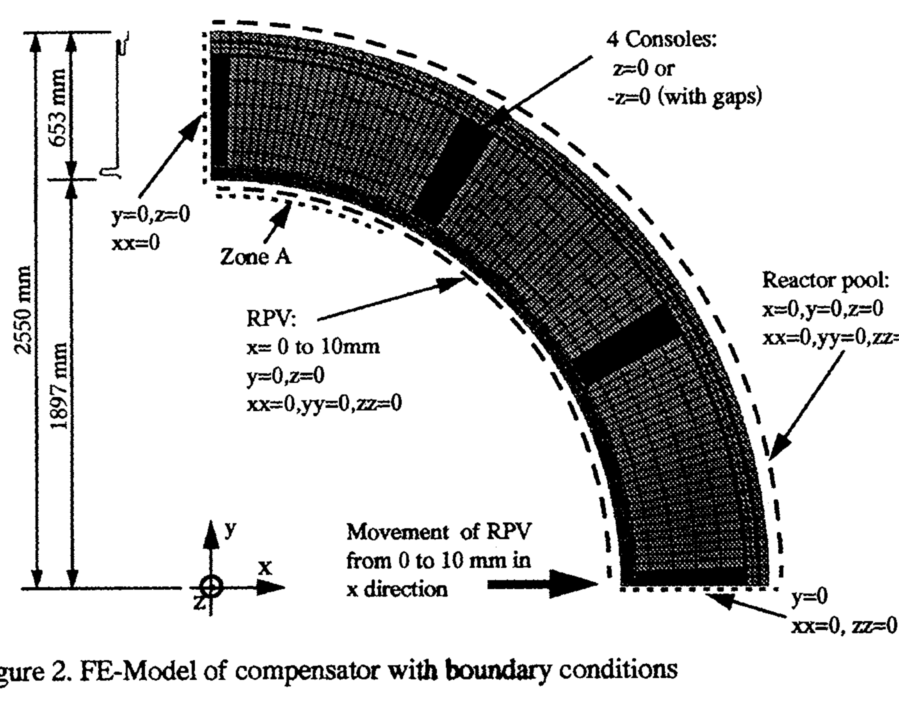


Figure 2. FE-Model of compensator with boundary conditions

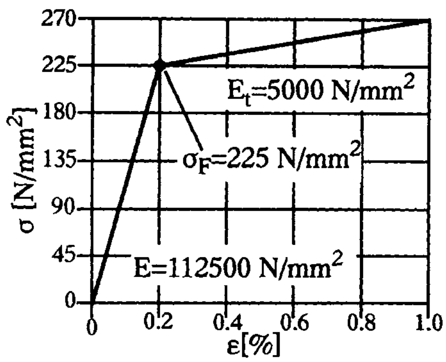


Figure 3. Stress-strain relation

## 3 ANALYSES

### 3.1 Variants of Analysis

Proceeding from a linear analysis the behaviour of the compensator system with variously combined bases for the analyses (linear buckling, linear or nonlinear material behaviour, large deformations, predeformations, use of gap elements) is investigated. In table 1 the accomplished static analyses A-F are summarized, including information on the bases for these analyses. Corresponding to the individual bases for the analyses the

| | Case | | | | | |
|---|---|---|---|---|---|---|
| | A | B | C | D | E | F |
| Stress-strain curve | linear | bilinear | linear | bilinear | bilinear | bilinear |
| Plastic strains | | x | | x | x | x |
| large deformation | | | x | x | x | x |
| Gap-elements | | | | | x | x |
| Predeformation | | | | | x | x |
| large deformation [mm] | 10,0 | 3.0 | 9.7 | 4,7 | 10,0 | 4,8 |
| Dead weight | | | | | | x |
| Buckling calculation | x | | | | | |

Table 1: Definition of the various analyses

respective basic system equations and the methods of analysis differ. In table 2 the basic equations of the various methods of analysis here applied are compared. For the analysis of the linear case A only the solution of the linear system of equations $\mathbf{F} = \mathbf{K}\ \mathbf{U}$ is necessary, whereas the belonging linear buckling analysis $(\mathbf{K} + \lambda \mathbf{K}_G)\ \mathbf{U} = \mathbf{0}$ requires the solution of an eigenvalue problem. Since with the nonlinear analyses B-F the system equations depend on the system displacements analyzed and on the sequence of loading an incremental solution of the problem is necessary. In every iteration step the stiffness matrix ${}^t\mathbf{K}$ resp. ${}_0^t\mathbf{K}_L$ changes, e. g. because of plastic strains appearing. Because of the change of the geometry of the building parts in consequence of the load applied ${}_0^t\mathbf{K}_{NL}$ is influenced. Here the full Newton-Raphson method is used for the necessary incremental used for the necessary incremental solution. Step by step the constraining displacement is increased up to the maximum value. A complete description of the methods applied is given in [1] and [2]. The analyses here presented were done with the NISA II finite-element program on an IBM RS6000/530H workstation. For the nonlinear analyses computing times between 12 to 48 CPU-hours were necessary, depending on the defined analysis and convergence parameters.

| Analysis and solution method | Basic equation |
|---|---|
| Linear<br>Linear system equation | $\mathbf{K}\,\mathbf{U} = \mathbf{F}$ |
| Linear buckling<br>Eigenvalue problem | $(\mathbf{K} + \lambda \mathbf{K}_G)\,\mathbf{U} = \mathbf{0}$ ; $\mathbf{K}_G = {}^t_o\mathbf{K}_{NL}$ |
| Material nonlinearity<br>iterative with Newton-Raphson | ${}^t\mathbf{K}\ \Delta\mathbf{U}^{(i)} = {}^{t+\Delta t}\mathbf{F} - {}^{t+\Delta t}\mathbf{P}^{(i-1)}$ |
| Material and geometry nonlinearity<br>(Total Lagrange)<br>iterative with Newton-Raphson | $\left({}^t_o\mathbf{K}_L + {}^t_o\mathbf{K}_{NL}\right)\Delta\mathbf{U}^{(i)} = {}^{t+\Delta t}\mathbf{F} - {}^{t+\Delta t}_{o}\mathbf{P}^{(i-1)}$ |

with:

- i .................. iteration step
- o .................. initial configuration
- t .............. time or load step
- $\Delta t$ ............ time (or load) increment
- $\mathbf{K}$ ................ linear stiffness matrix
- ${}^t\mathbf{K}$ .............. linear strain incremental stiffness matrix (no initial displacement effect)
- ${}^t_o\mathbf{K}_L$ ............ linear strain incremental stiffness matrix
- ${}^t_o\mathbf{K}_{NL}$, $\mathbf{K}_G$ .. initial stress or geometric stiffness matrix
- $\Delta\mathbf{U}$ ............. increment vector of node displacement
- $\mathbf{F}$ .................. vector of external node forces
- $\mathbf{P}$ ................ vector of internal node forces equivalent to element stresses

Table 2: Basic equations for the different analysis methods

## 3.2 Analysis Results

The stiffness of the compensator with respect to the displacements results from the sum of the reaction forces at all nodes at the inner edge (RPV connection). Figure 4 shows the change of the reaction forces via the constraining displacement for the various cases of analysis.

Case A: Naturally, the linear analysis results in a linear reaction force-displacement relation. This is the stiffest case. The belonging linear buckling analysis results in a failure of stability at the forced displacement of 9.7 mm. Local failure of buckling occurs at the inner edge in the area of the tangential flank of the compensator (cp. Figure 2, zone A).

Case B: With a forced displacement of approx. 1 mm plastification appears in the interior of the flank of the compensator (zone A). With an increase of the applied displacement this plastic zone extends along the inner edge. Figure 5 shows the development of the v. Mises equivalent stresses for the load steps 0.6 mm, 1.5 mm and 3 mm. The highest stresses are located at the inner expansion joint of the compensator (zone A) , where also the respective plastic strains appear. Since the stress-strain has been supposed to be bilinear the maximum stresses are higher than the yield point.

Case C: The analysis shows that with this model the consideration of the large deformations without the supposition of imperfections and material nonlinearities practically leads to the results of the linear analysis. The reaction force-displacement relation is linear and almost congruent to case A. At the displacement of 9.7 mm an abrupt collapse occurs, without any previous notice. This corresponds surprisingly exactly to the buckling load from case A.

Case D: The simultaneous consideration of material and geometrical nonlinearity practically leads to the identical results as case B (material nonlinearity only). The consideration of the large deformations is of no remarkable influence as well as in case C.

Cases E+F: If in addition to case D the possibility of the uplift at the consoles is considered with gap elements and if an imperfection of approx. 5 mm and a length of aprrox. 340 mm is applied in the region of buckling to be expected according to case A (zone A, cp. Figure 2), this leads to a stiffness which is a little less compared to that for the cases B and D, as shown in Figure 4. The influence of dead weight (case F) is unimportant.. However, it is interesting that contrary to the buckling analysis (case A) and to the geometrically nonlinear analysis (case C) the limit displacement of 10 mm is reached without the structure collapsing. The yielding of the material in the region of the first buckling leads to a redistribution of load which with a lower stiffness of the compensator system allows a higher deformation.

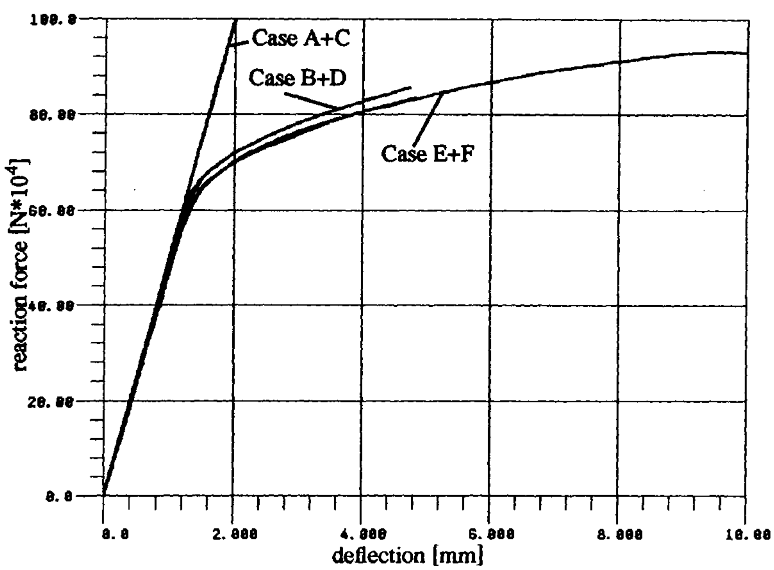


Figure 4. Reaction force versus RPV-deflection in x-direction

## 4 SUMMARY

The analyses as carried out at the compensator demonstrate that for an estimation of the

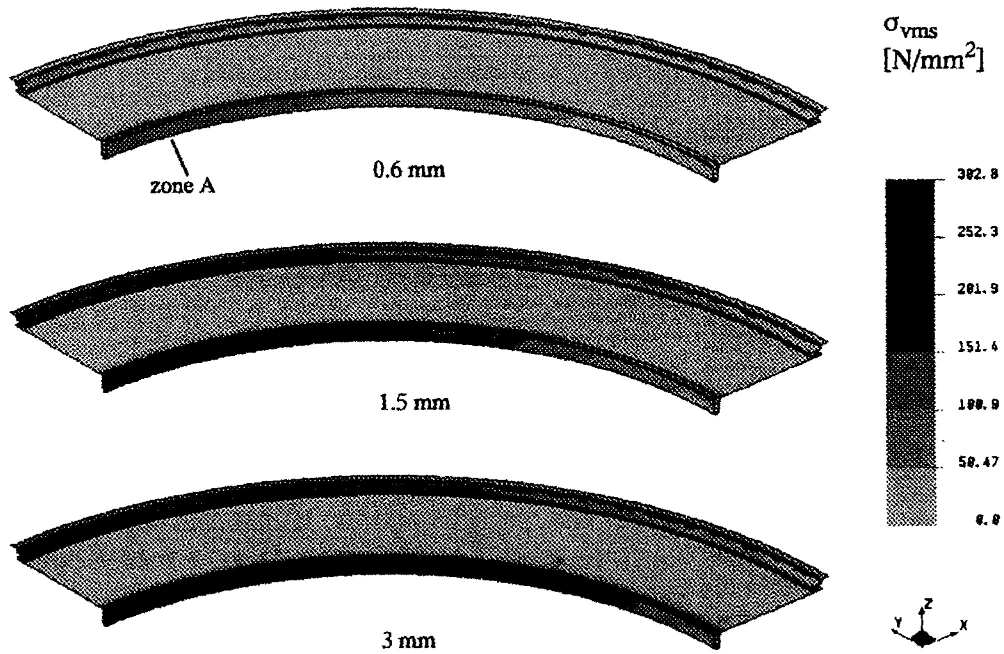


Figure 5. Case B, v.Mises Stress, RPV deflection 0,6mm, 1.5mm and 3.0 mm

system behaviour, particularly with larger deformations, nonlinear analyses supply informative knowledge that can be verified by engineering judgement. Basically, the stiffness of the system in the horizontal direction is influenced by zone A of the interior expansion joint of the compensator. If this region plastificates the reaction force increases only slightly, while this increase mainly depends on the plastic elasticity modulus $E_t$. Geometric imperfections and failure of stability have little influence on the load bearing behaviour. Therefore, without consideration of the nonlinear material behaviour the linear analysis and the analysis of stability as well as the geometrically nonlinear analysis result in a considerable increase of the stiffness of the system.

## REFERENCES

[1] Engineering Mechanics Research Corporation (EMRC). 1994. NISA II User‘s Manual. Troy, Michigan USA

[2] Bathe, K.-J. 1982. Finite Element Procedures in Engineering Analyses. Prentice-Hall, Englewood Cliffs, New Jersey